BIOLOGY, MEDICINE, & NATURAL PRODUCT CHEMISTRY ISSN 2089-6514 (paper)
Volume 15, Number 1, April 2026 | Pages: 411-420 | DOI: 10.14421/biomedich.2026.151.411-420 ISSN 2540-9328 (online)

Multi-Conformation Docking and Molecular Dynamics Study of Neolignan Compounds from *Ocimum sanctum* L. Targeting Estrogen Receptor Alpha

Fawwaz Muhammad Fauzi, Desti Kameliani
Department of Biotechnology, UIN Siber Syekh Nurjati Cirebon,
Jl. Perjuangan ByPass Sunyaragi, Kesambi, Kota Cirebon 45131, Indonesia.

Corresponding author*
fawwazmf@uinssc.ac.id

Manuscript received: 14 January 2026. Revision accepted: 13 April 2026, Published: 04 May 2026.

Abstract

Estrogen receptor alpha (ERα)-mediated breast cancer is the main target of hormone therapy. However, the long-term use of Selective Estrogen Receptor Modulators (SERMs) however, can lead to side effects and resistance. This study evaluated how well selected phenolic derivatives from *Ocimum sanctum* L. to various ERα conformations and to assess the initial stability of selected ligand-receptor complexes *in silico*. Five compounds, dominated by the neolignan group with one flavonoid derivative, were molecularly docked against four ERα structures representing the apo, agonist, and SERM states using AutoDock-GPU, with method validation through co-crystal ligand redocking. The binding affinity and key residue interactions were analyzed to assess cross-conformation consistency. The most stable ligand candidates were further analyzed using molecular dynamics simulations for 30 ns in the agonist and SERM conformations to evaluate the initial structural stabilities of the protein–ligand complexes. The docking results showed that most compounds had ERα conformation-dependent affinity; however, Tulsinol D exhibited the most consistent affinity profile and maintained interactions with key ERα residues across all tested conformations. Molecular dynamics simulations showed that the ERα–Tulsinol D complex had good initial stability, characterized by protein backbone stability, reasonable residue flexibility, maintained structural compactness, and stable ligand positioning within the binding pocket. Based on these results, Tulsinol D has potential as an in silico candidate inhibitor of ERα based on phenolic metabolites from *O. sanctum* and warrants further investigation through advanced computational studies and experimental validation.

Keywords: Estrogen receptor alpha; *in silico* study; molecular dynamics simulation; neolignan; *Ocimum sanctum* L.

INTRODUCTION

Breast cancer is one of the leading causes of death among women globally, and most cases are triggered by the activation of estrogen receptor alpha (ERα), which plays an important role in regulating cancer cell proliferation and survival (Bray et al., 2024; Wu et al., 2025). Owing to its critical role, ERα has become one of the primary therapeutic targets in developing breast cancer drugs using Selective Estrogen Receptor Modulators (SERMs), such as tamoxifen and its derivatives (Linowiecka et al., 2024). Although clinically effective, SERM-based therapy has been reported to cause various side effects and resistance with long-term use, prompting the exploration of safer and more selective alternative ERα inhibitors (Buijs et al., 2024; Gautam et al., 2025; Mills et al., 2018).

Ocimum sanctum L. is rich in secondary metabolites, including phenolic derivatives such as flavonoids and neolignans, which have been reported to exhibit various pharmacological activities, including antioxidant, anticancer, anti-inflammatory, and leishmanicidal properties (Bhattarai et al., 2024; Hasan et al., 2023; Suzuki et al., 2009). Initial in silico studies have indicated that several neolignan and flavonoid derivatives have a competitive affinity for ERα and interact with the ligand-binding domain (LBD) (Fauzi et al., 2024). This finding provides an opportunity to further evaluate the potential of neolignans and flavonoids from *O. sanctum* as a candidate ERα inhibitor.

However, ligand–receptor interactions at ERα are complex because this receptor has several functional conformations, such as agonist, antagonist, and apo states, which are indicated to have an influence on the characteristics of the binding pocket and the mode of ligand interaction, such as the positional shift of helix 12 (H12) and changes in the interaction landscape (McDougal et al., 2025). Therefore, evaluating ligand candidates against a single ER-α conformation has the potential to produce structural bias and is insufficient for comprehensively assessing the consistency of ligand-binding ability.

This study further evaluated selected phenolic compounds from *O. sanctum* using a molecular docking approach on several ER-α structures representing different biological states, namely SERM, agonist, and apo conformations. This approach was used to assess the consistency of binding affinity and the pattern of interaction of key residues across receptor conformations so that the identified ligand candidates not only show superior performance on a specific protein structure.

The multi-conformation docking results guided the selection of consistent ligand candidates for molecular dynamics (MD) simulations. Hollingsworth & Dror (2018) stated that MD simulation is an important approach in *in silico* validation to evaluate the initial stability of protein-ligand complexes in a soluble environment and under thermodynamic conditions that are closer to physiological conditions. Considering computational resource limitations, simulations were performed over a short time scale and focused on the two main functional states of ER-α, namely, the SERM and agonist states.

Based on this approach, the objective of this study was to evaluate the consistency of the binding ability of selected neolignan compounds from *O. sanctum* to various ER-α conformations through multi-structure docking and, as well as to assess the initial stability of selected ligand candidates in SERM and ER-α agonist states using short-term molecular dynamics simulations. This study is expected to strengthen the scientific basis for the development of ERα inhibitor candidates based on phenolic metabolites derived from *O. sanctum*.

MATERIALS AND METHODS

Materials and Data Sources

The structures of neolignan and flavonoid compounds in *Ocimum sanctum* L. (tulsinols A, B, C, D, and G) were obtained from the KNApSAcK database (Afendi et al., 2012). The structure of the estrogen receptor alpha (ERα) protein was downloaded from the Protein Data Bank (PDB) (Berman, 2000), including 3ERT, 2OUZ, 1A52, and 1G50 (Eiler et al., 2001; Shiau et al., 1998; Tanenbaum et al., 1998; Vajdos et al., 2007). The ligand structures were optimized using Avogadro software (Hanwell et al., 2012).

Procedures

Protein and ligand preparation

The proteins were cleaned of water molecules, ions, and co-crystal ligands. Polar hydrogen atoms were added, and partial charges were calculated using AutoDockTools 1.5.7 (Santos-Martins et al., 2021). The structures of the ligands (tulsinols A, B, C, D, and G) and reference ligands (estradiol, 4-hydroxytamoxifen, and lasofoxifene) were geometrically optimized and Gasteiger charges were assigned before being saved as PDBQT files (Jablonský et al., 2022).

Molecular docking

The docking procedure was validated by redocking the co-crystal ligand into the binding pocket of each protein. The method was considered valid if the root mean square deviation (RMSD) value between the redocked ligand and crystallographic ligand was < 2.0 Å (Fauzi et al., 2024; Mora Lagares et al., 2020).

Docking was performed using AutoDock-GPU, which implements the Lamarckian Genetic Algorithm-based AutoDock4 scoring function (Santos-Martins et al., 2021). A grid box was set to cover the entire ligand-binding domain (LBD) in each ERα structure. Docking parameters (grid size, number of evaluations, and number of runs) were standardized for all ligands so that the results could be compared consistently. The best pose was selected based on the lowest binding energy and evaluated using BIOVIA Discovery Studio Visualizer to identify hydrogen bonds, hydrophobic interactions, and key ligand-binding domain (LBD) interacting residues (BIOVIA, 2025).

Molecular dynamics simulation

Selected protein-ligand complexes resulting from docking evaluation were prepared using CHARMM-GUI (Lee et al., 2020). Proteins were parameterized using AMBER FF19SB, whereas ligands were parameterized using GAFF2 with AM1-BCC charges (He et al., 2020; Tian et al., 2020). The system was placed in a cubic simulation box, solvated with the TIP3P water model (Jorgensen et al., 1983), and neutralized using Na^+ and Cl^- ions to achieve neutral conditions with physiological ionic strength (Lee et al., 2020).

Simulations were performed using GROMACS 2025.4 (M. Abraham et al., 2025; M. J. Abraham et al., 2015). Each system was first minimized using the steepest descent algorithm until the convergence criteria were met. This was followed by an equilibration stage following the CHARMM-GUI protocol at a temperature of 310 K and pressure of 1 bar with the application of an appropriate thermostat and barostat (Lee et al., 2020). The next stage was a production simulation for 30 ns to obtain the molecular dynamics trajectory used in the analysis.

Trajectory analysis

Analysis of molecular dynamics simulation trajectories was performed using the built-in utilities of the GROMACS software package. Various structural parameters were analyzed along the simulation trajectories, including the root mean square deviation (RMSD) of the protein backbone and the RMSD of the ligand relative to the initial simulation structure.

Protein residue fluctuations during simulation were analyzed using root mean square fluctuation (RMSF) backbone. The level of compactness of protein structure was analyzed by calculating radius of gyration (Rg) based on protein backbone coordinates. Solvent-

accessible surface area (SASA) of the proteins was calculated along the simulation trajectory. Noncovalent interactions between proteins and ligands were analyzed by calculating the number of hydrogen bonds along the trajectory.

All trajectory analyses were performed using the gmx rmsd, gmx rmsf, gmx gyrate, gmx sasa, and gmx hbond modules integrated into the GROMACS software package (M. Abraham et al., 2025; M. J. Abraham et al., 2015). The trajectory analysis data were then visualized in a graphical form using Python scripts based on the matplotlib library (Hunter, 2007).

RESULTS AND DISCUSSION

Molecular docking result

The validity of the docking procedure was evaluated by redocking the co-crystal ligands into the binding pockets of each estrogen receptor alpha (ERα) structure. The redocking results showed that the docking poses of the ligands could be reproduced well, with root mean square deviation (RMSD) values of 1.53 Å for the 3ERT structure, 0.92 Å for 2OUZ, 0.94 Å for 1A52, and 0.91 Å for 1G50. All RMSD values were below the threshold of 2.0 Å, indicating that the docking parameters and settings used were adequate for predicting the ligand binding mode on the ERα ligand-binding domain (LBD).

Table 1. Docking binding energies of tulsinol compounds from Ocimum sanctum L. against ERα in different conformational states

Ligand	Binding energy (kcal/mol)			
	3ERT	2OUZ	1A52	1G50
4-hydroxytamoxifen	-10.35	-	-	-
Lasofoxifene	-	-13.48	-	-
Estradiol	-	-	-10.46	-10.60
Tulsinol A	-10.88	-11.10	-11.14	-9.09
Tulsinol B	-13.48	-13.03	-13.97	-3.87
Tulsinol C	-13.31	-14.00	-14.17	-11.27
Tulsinol D	-13.15	-14.46	-14.68	-13.71
Tulsinol G	-10.96	-11.07	-11.07	-12.37

The results of molecular docking of the reference ligand and tulsinol compounds from *Ocimum sanctum* L. against ERα in various conformations are presented in Table 1 and Figure 1. All tulsinol compounds were able to bind to the LBD of ERα, but showed variations in binding affinity depending on the receptor conformation. The reference ligands exhibited affinity patterns consistent with their biological functions, where 4-hydroxytamoxifen and lasofoxifene showed high affinity in the SERM conformation, while estradiol had stable affinity in the agonist and apo conformations.

Among all docked compounds, Tulsinol D showed relatively low and consistent binding energy values across all ERα conformations used. In contrast, other tulsinol compounds showed high affinity only in certain conformations and decreased affinity for other conformations.

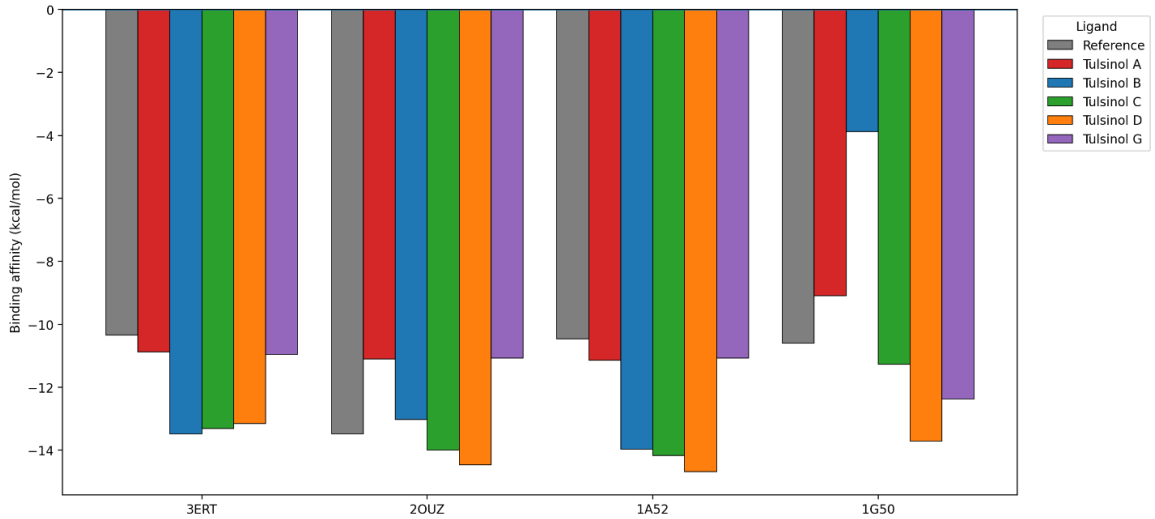

Figure 1. Docking binding energies of tulsinol compounds from *O. sanctum* against ERα across different conformations.

Analysis of ligand interactions with key ERα residues, including Glu353, Arg394, and His524, is presented in Table 2. The reference ligand maintained interactions with these residues in conformations that were consistent with their roles. Most tulsinol compounds exhibit inconsistent residue interaction patterns, that appear only in certain conformations, or are dominated by hydrophobic interactions. However, Tulsinol D maintains engagement with all three key residues in all ERα conformations tested, with a combination of hydrogen bonding and hydrophobic interactions.

Two-dimensional visualization of ligand–protein interactions showed that Tulsinol D occupied the same ERα binding pocket as the reference ligand and interacted with canonical ERα LBD residues (Figure 2). Based on the consistency of binding affinity and the pattern of key residue interactions across conformations, Tulsinol D was selected as a candidate ligand for further analysis using molecular dynamics simulations.

Table 2. Consistency of ligand interactions with key ERα residues across conformations.

Ligand	ERα key residue		
	Glu353	**Arg394**	**His524**
4-hydroxytamoxifen	3ERT (HB)	3ERT (HB)	3ERT (HI)
Lasofoxifene	2OUZ (HB)	2OUZ (HB)	2OUZ (HI)
Estradiol	1A52 (HB), 1G50 (HB)	1A52 (HB), 1G50 (HB)	1A52 (HB), 1G50 (HB)
Tulsinol A	1A52 (HI), 1G50 (HI), 2OUZ (HB), 3ERT (HB)	1A52 (HI), 1G50 (HI), 2OUZ (HB), 3ERT (HB)	1A52 (HB), 1G50 (HI), 2OUZ (HI), 3ERT (HB)
Tulsinol B	1A52 (HI), 2OUZ (HI), 3ERT (HI)	1A52 (HI), 1G50 (HI), 2OUZ (HI), 3ERT (HI)	1A52 (HI), 1G50 (HI), 2OUZ (HB), 3ERT (HI)
Tulsinol C	1G50 (HI), 3ERT (HI)	1G50 (HI), 3ERT (HI)	1A52 (HI), 1G50 (HI), 2OUZ (HI), 3ERT (HI)
Tulsinol D	1A52 (HI), 1G50 (HB), 2OUZ (HB), 3ERT (HI)	1A52 (HI), 1G50 (HB), 2OUZ (HB), 3ERT (HI)	1A52 (HB), 1G50 (HI), 2OUZ (HI), 3ERT (HI)
Tulsinol G	1A52 (HB), 1G50 (HI), 2OUZ (HB), 3ERT (HB)	1A52 (HI), 1G50 (HI), 2OUZ (HI), 3ERT (HI)	1A52 (HB), 1G50 (HI), 2OUZ (HI), 3ERT (HB)

Note: HB= Hydrogen bond; HI= Hydrophobic interaction

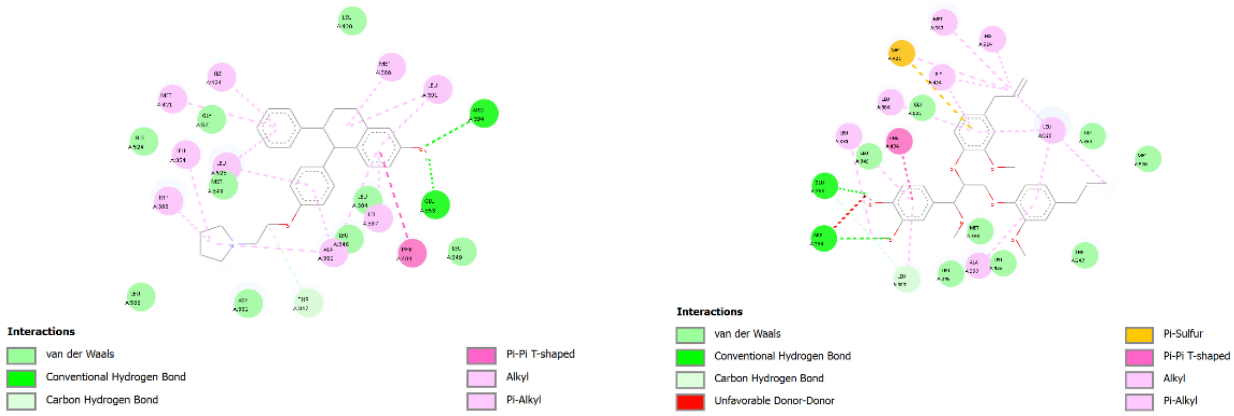

(a) (b)

Figure 2. 2D interaction diagrams of (a) reference ligand and (b) Tulsinol D within the ligand-binding domain of ERα (PDB ID: 2OUZ).

Molecular dynamics simulation result

Molecular dynamics simulations were performed on the ERα–Tulsinol D complex in the SERM (2OUZ) and agonist (1G50) conformations for 30 ns, and compared with the respective reference ligand complexes. The initial stability of the protein–ligand complexes was evaluated by analyzing the backbone RMSD, RMSF, radius of gyration (Rg), ligand RMSD, solvent-accessible surface area (SASA), and number of hydrogen bonds.

The backbone RMSD profile showed an initial increase in the early phase of the simulation, reflecting the relaxation process of the structure from its crystalline state, followed by relatively stable conditions in both ERα conformations (Figure 3). In the agonist conformation (1G50), the backbone RMSD values of the ERα–estradiol complex were in the range of 0.10–0.22 nm, while those of the ERα–Tulsinol D complex were in the range of 0.11–0.21 nm throughout the 30 ns simulation, with moderate fluctuations and no extreme spikes. In the SERM conformation (2OUZ), the ERα–lasofoxifene and ERα–Tulsinol D complexes showed higher backbone RMSD values than the agonist conformation, ranging from 0.15 to 0.34 nm and 0.15 to 0.30 nm, respectively. Although the backbone RMSD fluctuations in both complexes were greater, the RMSD values remained within a controlled range and did not exhibit a continuous upward trend until the end of the simulation.

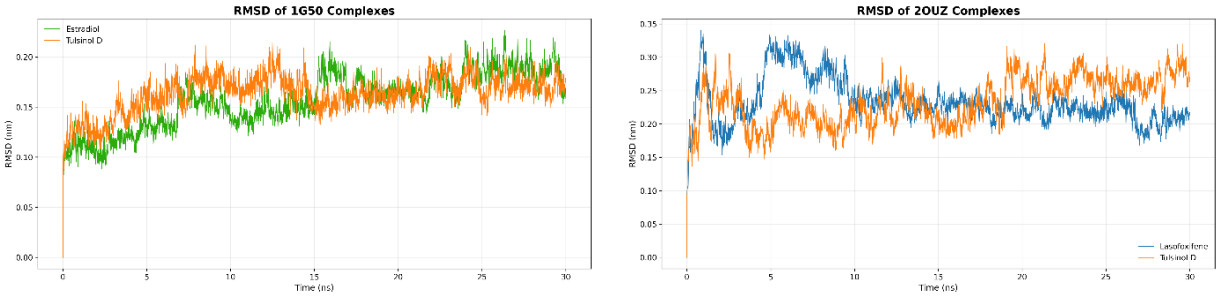

(a) (b)

Figure 3. Backbone RMSD of ERα–ligand complexes in (a) agonist (PDBID: 1G50) and (b) SERM (PDBID: 2OUZ) conformations during 30 ns molecular dynamics simulations.

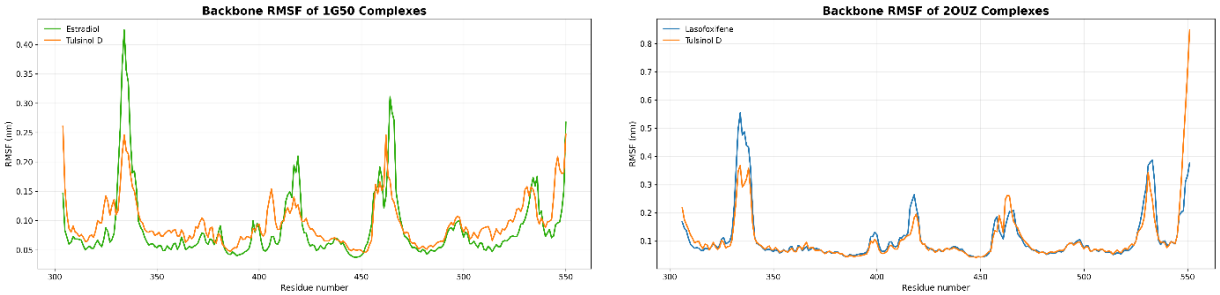

(a) (b)

Figure 4. Backbone RMSF of ERα–ligand complexes in (a) agonist (PDBID: 1G50) and (b) SERM (PDBID: 2OUZ) conformations during 30 ns molecular dynamics simulations.

Root mean square fluctuation (RMSF) analysis of the backbone was performed to evaluate the flexibility of ERα residues during molecular dynamics simulations. Specifically, in the agonist conformation (1G50), most residues in the ERα–Tulsinol D and ERα–estradiol complexes showed RMSF values in the range of 0.05–0.15 nm, with some local fluctuation peaks reaching approximately 0.25 nm for Tulsinol D and 0.42 nm for estradiol (Figure 4). In the SERM conformation (2OUZ), the majority of residues showed RMSF values in the range of 0.06–0.12 nm, with local fluctuation peaks reaching approximately 0.35–0.38 nm in the ERα–Tulsinol D complex and up to 0.55 nm in the reference ligand complex. These high fluctuations were local and not widely distributed along the protein domain.

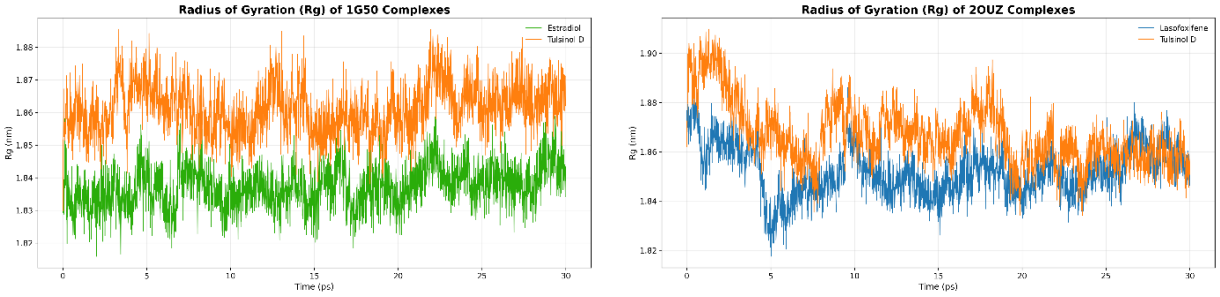

(a) (b)

Figure 5. Radius of gyration of ERα–ligand complexes in (a) agonist (PDBID: 1G50) and (b) SERM (PDBID: 2OUZ) conformations during 30 ns molecular dynamics simulations.

Based on Figure 5, the radius of gyration (Rg) profile shows that the global structure of ERα remained compact throughout the simulation. In the agonist conformation (1G50), the Rg value of the ERα–estradiol complex was in the range of 1.82–1.85 nm, while the ERα–Tulsinol D complex was in the range of 1.85–1.88 nm, with fluctuations of less than 0.06 nm throughout the simulation. Meanwhile, in the SERM conformation

(2OUZ), the Rg values of the ERα–lasofoxifene and ERα–Tulsinol D complexes were in the range of 1.83–1.87 nm and 1.85–1.90 nm, respectively, with relatively small fluctuations (< 0.07 nm) and no long-term upward or downward trends.

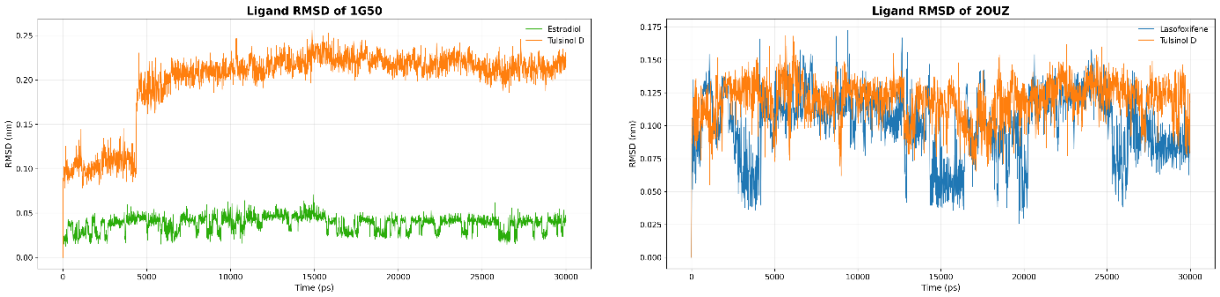

(a) (b)

Figure 6. Ligand RMSD of ERα–ligand complexes in (a) agonist (PDBID: 1G50) and (b) SERM (PDBID: 2OUZ) conformations during 30 ns molecular dynamics simulations.

The ligand RMSD analysis shown in Figure 6 indicates that the ligand remained within the ERα binding pocket throughout the simulation. In the agonist conformation (1G50), estradiol maintained a low and stable ligand RMSD in the range of 0.02–0.06 nm. In contrast, Tulsinol D showed an increase in RMSD in the early phase of the simulation, followed by a plateau condition in the range of 0.18–0.24 nm until the end of the simulation. In the SERM conformation (2OUZ), the RMSD of lasofoxifene and Tulsinol D ligands showed relatively similar fluctuations, ranging from 0.05–0.15 nm and 0.10–0.15 nm, respectively, without any extreme RMSD spikes or significant ligand position shifts.

Figure 7 shows the solvent-accessible surface area (SASA) profile of the protein, which fluctuated slightly throughout the simulation in both conformations. In the agonist conformation (1G50), the SASA value of the ERα–estradiol complex ranged from 122 to 130 nm^2, while that of the ERα–Tulsinol D complex ranged from 125 to 135 nm^2. In the SERM conformation (2OUZ), the ERα–lasofoxifene complex showed SASA values in the range of 128–142 nm^2, while the ERα–Tulsinol D complex was in the range of 132–145 nm^2. No consistent upward or downward trend in SASA was observed during the simulation.

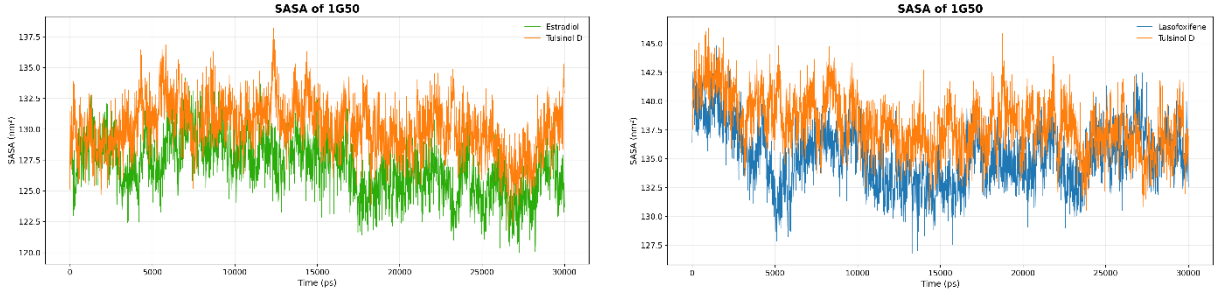

(a) (b)

Figure 7. SASA of Protein of ERα–ligand complexes in (a) agonist (PDBID: 1G50) and (b) SERM (PDBID: 2OUZ) conformations during 30 ns molecular dynamics simulations.

The number of hydrogen bonds between ligands and ERα fluctuated throughout the molecular dynamics simulation (Figure 8). In the agonist conformation (1G50), estradiol formed 0–3 hydrogen bonds, while Tulsinol D generally formed 0–1 hydrogen bonds with a lower frequency. In the SERM conformation (2OUZ), lasofoxifene forms 0–2 hydrogen bonds, while Tulsinol D shows a fluctuating number of hydrogen bonds in the range of 0–3, with sporadic appearances of up to four hydrogen bonds in some simulation intervals.

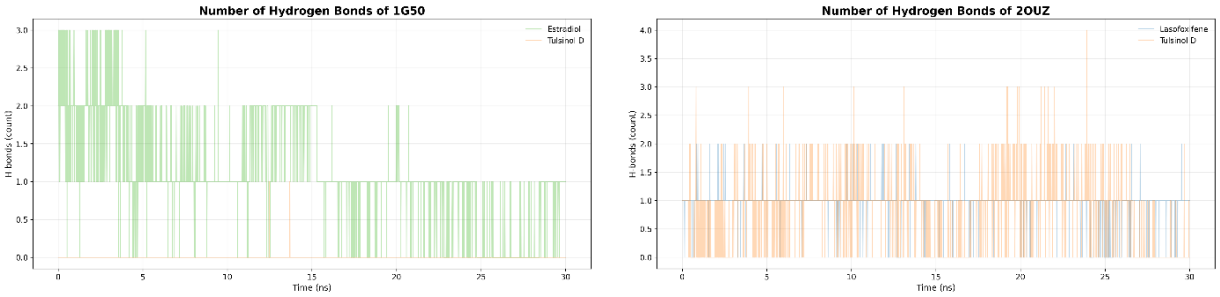

(a) (b)

Figure 8. Number of Hydrogen Bonds of ERα–ligand complexes in (a) agonist (PDBID: 1G50) and (b) SERM (PDBID: 2OUZ) conformations during 30 ns molecular dynamics simulations.

Discussion

The multi-conformation docking approach in this study confirmed that ligand performance against estrogen receptor alpha (ERα) cannot be assessed based on a single protein structure state, given that ERα is a nuclear receptor with a dynamic ligand binding domain (LBD) that adopts conformational changes, such as apo, agonist, and SERM states (Fanning et al., 2018; McDougal et al., 2025). This was reflected in the docking results (Table 1 and Figure 1), where most tulsinol compounds showed ERα conformation-dependent affinity. In contrast, Tulsinol D maintained a relatively consistent binding affinity across all tested conformations. This consistency is reinforced by the analysis of key residue interactions (Table 2), which showed the involvement of Glu353, Arg394, and His524 in all ERα conformations. These residues are widely reported as canonical residues that play an important role in ligand binding and stabilization of the ERα ligand-binding domain (Dubey et al., 2025; Masand et al., 2024). Thus, from a structural perspective, Tulsinol D exhibits a relatively consistent binding mode across variations in the microenvironment of the ERα binding pocket.

Dynamic validation through molecular dynamics simulations contextualizes these docking findings. Backbone RMSD analysis (Figure 3) showed that the ERα–Tulsinol D complex maintained global structural stability comparable to the reference ligand in both ERα states analyzed. In the agonist conformation (1G50), the backbone RMSD range of the ERα–Tulsinol D complex (0.11–0.21 nm) was nearly identical to that of ERα–estradiol (0.10–0.22 nm), while in the SERM conformation (2OUZ), the backbone RMSD values of ERα–Tulsinol D (0.15–0.30 nm) were also within a range comparable to ERα–lasofoxifene (0.18–0.33 nm). In general, a relatively stable backbone RMSD without a continuous upward trend was interpreted as an indicator of no progressive global conformational deviation during the simulation (Hassan et al., 2024; Zhang & Lazim, 2017). The relatively higher RMSD values in SERM conformations compared to agonists are consistent with the structural characteristics of ERα, which are generally reported to involve different ligand-binding domain (LBD) configurations, including the orientation of helix-12 (McDougal et al., 2025).

RMSF backbone analysis (Figure 4) provides a more detailed picture of residue flexibility during simulation. In the agonist conformation (1G50), most residues in the ERα–Tulsinol D complex were in the range of 0.05–0.15 nm, with a peak local fluctuation of approximately 0.25 nm, which was still lower than the peak fluctuation in the ERα–estradiol complex (~0.42 nm). A similar pattern was observed in the SERM conformation (2OUZ), where the local RMSF peak in the ERα–Tulsinol D complex (~0.35–0.38 nm) was lower than that of the reference ligand, which reached ~0.55 nm. Conceptually, local RMSF peaks are generally associated with intrinsically flexible protein loops or segments, whereas the stability of the core domain is reflected in relatively low and uniform residue fluctuations (Hassan et al., 2024; Yusuff et al., 2023). This indicates that Tulsinol D binding does not trigger a widespread increase in residue flexibility in the ERα LBD.

The global stability of the protein is also reflected in the radius of gyration (Rg) profile (Figure 5), where Rg fluctuations in both conformations are relatively small (<0.06–0.07 nm) and do not show any long-term increasing or decreasing trends. A stable Rg is generally interpreted as an indicator that the protein structure remains compact and does not undergo major conformational changes during molecular dynamics simulations (Hassan et al., 2024). Thus, the RMSD, RMSF, and Rg data collectively support the initial stability of the ERα–Tulsinol D complex in a soluble environment.

Ligand position stability within the binding pocket was evaluated using ligand RMSD (Figure 6). In the agonist conformation (1G50), estradiol maintained a low and stable ligand RMSD (0.02–0.06 nm), while Tulsinol D showed an initial adaptation phase before reaching a plateau in the range of 0.18–0.24 nm. The plateau in ligand RMSD after the initial phase is generally interpreted as an adjustment in ligand orientation to achieve a local minimum energy state compatible with the binding pocket, rather than as an indication of ligand release from the receptor (Salmaso & Moro, 2018). This is supported by the results in the SERM conformation

(2OUZ), where the RMSD of the Tulsinol D ligand (0.10–0.15 nm) remained within a range comparable to that of the reference ligand lasofoxifene and did not show a progressive drifting pattern.

The solvent-accessible surface area (SASA) profile of the protein (Figure 7) showed slight fluctuations around the average value without a consistent upward or downward trend. In both agonist and SERM conformations, the SASA range of the ERα–Tulsinol D complex was comparable to that of the reference ligand complex. In the context of molecular dynamics simulations, the absence of a sharp increase in SASA is often used as an indicator of the absence of opening of the protein structure or major changes in surface exposure to the solvent (Hassan et al., 2024).

Analysis of the number of hydrogen bonds (Figure 8) showed that the ligand–ERα interaction was dynamic and fluctuated throughout the simulation. In the agonist conformation, Tulsinol D forms fewer hydrogen bonds than estradiol, whereas in the SERM conformation, the number of Tulsinol D hydrogen bonds was comparable to that of the reference ligand and showed sporadic appearance of additional hydrogen bonds. In the context of nuclear receptors, a relatively low number of hydrogen bonds does not automatically indicate an unstable complex, because hydrophobic interactions play a dominant role in stabilizing ligands within the ERα ligand-binding domain (Masand et al., 2024; Yao et al., 2023).

The integration of multi-conformation docking results (Tables 1–2; Figures 1–2) and short-term molecular dynamics simulations (Figures 3–8) shows that Tulsinol D has consistent binding ability to ERα and initial protein–ligand complex stability comparable to reference ligands in agonist and SERM states. However, given that the simulation duration is still limited to 30 ns, these findings are best interpreted as an indication of initial stability, rather than long-term stability or direct biological potential (Genheden & Ryde, 2015). Therefore, longer molecular dynamics simulations and trajectory-based binding energy estimates, such as MM/PBSA and MM/GBSA, are recommended to strengthen the energetic evaluation and deepen the understanding of the binding mechanism of Tulsinol D to ERα.

CONCLUSIONS

The affinity binding evaluation and key residue interaction patterns based on multi-structure docking studies of various ER-α conformations (apo, agonist, and SERM) of selected neolignan and flavonoid compounds from *Ocimum sanctum* L showed that Tulsinol D was the most promising computational ligand candidate, based on its binding affinity values and interactions with key residues in various conformations. Short-term molecular dynamics simulations showed that the ERα–Tulsinol D complex was relatively stable in the agonist and SERM conformations, with the protein structure and ligand position stayed stable throughout the simulation. These results support the potential of Tulsinol D as a candidate *in silico* natural-based ER-α modulator.

Further research should focus on longer-time-scale molecular dynamics simulations to evaluate the stability of the ERα–Tulsinol D complex over a more biologically representative time frame. Further analyses such as MM/GBSA or MM/PBSA calculations can be performed to strengthen binding affinity estimates. This computational approach can be combined with the exploration of Tulsinol D derivatives or related phenolic compounds to identify candidates with optimal interaction profiles prior to experimental validation.

Acknowledgements: The author gratefully acknowledges that this research was conducted independently without external financial or institutional support.

Authors' Contributions: The author conceived and designed the study, performed computational analysis, interpreted the data, and wrote the manuscript.

Competing Interests: The author declares that there are no competing interests.

Funding: This study received no external funding.

REFERENCES

Abraham, M., Alekseenko, A., Andrews, B., Basov, V., Bauer, P., Bird, H., Briand, E., Brown, A., Doijade, M., Fiorin, G., Fleischmann, S., Gorelov, S., Gouaillardet, G., Gray, A., Irrgang, M. E., Jalalypour, F., Johansson, P., Kutzner, C., Łazarski, G., … Lindahl, E. (2025). *GROMACS Documentation Release 2025.4 GROMACS development team*.

Abraham, M. J., Murtola, T., Schulz, R., Páll, S., Smith, J. C., Hess, B., & Lindahl, E. (2015). GROMACS: High performance molecular simulations through multi-level parallelism from laptops to supercomputers. *SoftwareX*, *1–2*, 19–25. https://doi.org/10.1016/j.softx.2015.06.001

Afendi, F. M., Okada, T., Yamazaki, M., Hirai-Morita, A., Nakamura, Y., Nakamura, K., Ikeda, S., Takahashi, H., Altaf-Ul-Amin, Md., Darusman, L. K., Saito, K., & Kanaya, S. (2012). KNApSAcK Family Databases: Integrated Metabolite–Plant Species Databases for Multifaceted Plant Research. *Plant and Cell Physiology*, *53*(2), e1–e1. https://doi.org/10.1093/pcp/pcr165

Berman, H. M. (2000). The Protein Data Bank. *Nucleic Acids Research*, *28*(1), 235–242. https://doi.org/10.1093/nar/28.1.235

Bhattarai, K., Bhattarai, R., Pandey, R. D., Paudel, B., & Bhattarai, H. D. (2024). A Comprehensive Review of the Phytochemical Constituents and Bioactivities of Ocimum tenuiflorum. *TheScientificWorldJournal*, *2024*, 8895039. https://doi.org/10.1155/2024/8895039

BIOVIA. (2025). *BIOVIA Discovery Studio Visualizer 2025*. Dassault Systèmes.

Bray, F., Laversanne, M., Sung, H., Ferlay, J., Siegel, R. L., Soerjomataram, I., & Jemal, A. (2024). Global cancer statistics 2022: GLOBOCAN estimates of incidence and mortality worldwide for 36 cancers in 185 countries. *CA: A Cancer Journal for Clinicians*, *74*(3), 229–263. https://doi.org/10.3322/caac.21834

Buijs, S. M., Koolen, S. L. W., Mathijssen, R. H. J., & Jager, A. (2024). Tamoxifen Dose De-Escalation: An Effective Strategy for Reducing Adverse Effects? *Drugs*, *84*(4), 385–401. https://doi.org/10.1007/s40265-024-02010-x

Dubey, A., Al-Lohedan, H. A., Ali, M. S., & Ragusa, A. (2025). Integrative in silico analysis to explore the potential of Zingiberaceae compounds to inhibit estrogen receptor alpha activity in breast cancer. *Journal of Molecular Graphics and Modelling*, *138*, 109023. https://doi.org/10.1016/j.jmgm.2025.109023

Eiler, S., Gangloff, M., Duclaud, S., Moras, D., & Ruff, M. (2001). Overexpression, Purification, and Crystal Structure of Native ERα LBD. *Protein Expression and Purification*, *22*(2), 165–173. https://doi.org/10.1006/prep.2001.1409

Fanning, S. W., Hodges-Gallagher, L., Myles, D. C., Sun, R., Fowler, C. E., Plant, I. N., Green, B. D., Harmon, C. L., Greene, G. L., & Kushner, P. J. (2018). Specific stereochemistry of OP-1074 disrupts estrogen receptor alpha helix 12 and confers pure antiestrogenic activity. *Nature Communications*, *9*(1), 2368. https://doi.org/10.1038/s41467-018-04413-3

Fauzi, F. M., Wutsqa, Y. U., & Rohmatika, N. A. (2024). Studi Bioavailabilitas Dan Molecular Docking Senyawa Fenolik Ocimum sanctum L. sebagai Inhibitor Reseptor Estrogen Alfa pada Sel Kanker Payudara. *Jurnal Kefarmasian Akfarindo*, *09*(01), 49–56. https://www.rcsb.org/structure/3ERT

Gautam, S., Maurya, R., Vikal, A., Patel, P., Thakur, S., Singh, A., Gupta, G. Das, & Kurmi, B. Das. (2025). Understanding drug resistance in breast cancer: Mechanisms and emerging therapeutic strategies. *Medicine in Drug Discovery*, *26*, 100210. https://doi.org/10.1016/j.medidd.2025.100210

Genheden, S., & Ryde, U. (2015). The MM/PBSA and MM/GBSA methods to estimate ligand-binding affinities. *Expert Opinion on Drug Discovery*, *10*(5), 449–461. https://doi.org/10.1517/17460441.2015.1032936

Hanwell, M. D., Curtis, D. E., Lonie, D. C., Vandermeersch, T., Zurek, E., & Hutchison, G. R. (2012). Avogadro: an advanced semantic chemical editor, visualization, and analysis platform. *Journal of Cheminformatics*, *4*(1), 17. https://doi.org/10.1186/1758-2946-4-17

Hasan, M. R., Alotaibi, B. S., Althafar, Z. M., Mujamammi, A. H., & Jameela, J. (2023). An Update on the Therapeutic Anticancer Potential of Ocimum sanctum L.: "Elixir of Life". *Molecules (Basel, Switzerland)*, *28*(3). https://doi.org/10.3390/molecules28031193

Hassan, A. M., Gattan, H. S., Faizo, A. A., Alruhaili, M. H., Alharbi, A. S., Bajrai, L. H., AL-Zahrani, I. A., Dwivedi, V. D., & Azhar, E. I. (2024). Evaluating the Binding Potential and Stability of Drug-like Compounds with the Monkeypox Virus VP39 Protein Using Molecular Dynamics Simulations and Free Energy Analysis. *Pharmaceuticals*, *17*(12), 1617. https://doi.org/10.3390/ph17121617

He, X., Man, V. H., Yang, W., Lee, T.-S., & Wang, J. (2020). A fast and high-quality charge model for the next generation general AMBER force field. *The Journal of Chemical Physics*, *153*(11), 114502. https://doi.org/10.1063/5.0019056

Hollingsworth, S. A., & Dror, R. O. (2018). Molecular Dynamics Simulation for All. *Neuron*, *99*(6), 1129–1143. https://doi.org/10.1016/j.neuron.2018.08.011

Hunter, J. D. (2007). Matplotlib: A 2D Graphics Environment. *Computing in Science & Engineering*, *9*(3), 90–95. https://doi.org/10.1109/MCSE.2007.55

Jablonský, M., Štekláč, M., Majová, V., Gall, M., Matúška, J., Pitoňák, M., & Bučinský, L. (2022). Molecular docking and machine learning affinity prediction of compounds identified upon softwood bark extraction to the main protease of the SARS-CoV-2 virus. *Biophysical Chemistry*, *288*, 106854. https://doi.org/10.1016/j.bpc.2022.106854

Jorgensen, W. L., Chandrasekhar, J., Madura, J. D., Impey, R. W., & Klein, M. L. (1983). Comparison of simple potential functions for simulating liquid water. *The Journal of Chemical Physics*, *79*(2), 926–935. https://doi.org/10.1063/1.445869

Lee, J., Hitzenberger, M., Rieger, M., Kern, N. R., Zacharias, M., & Im, W. (2020). CHARMM-GUI supports the Amber force fields. *The Journal of Chemical Physics*, *153*(3). https://doi.org/10.1063/5.0012280

Linowiecka, K., Szpotan, J., Godlewska, M., Gaweł, D., Zarakowska, E., Gackowski, D., Brożyna, A. A., & Foksiński, M. (2024). Selective Estrogen Receptor Modulators' (SERMs) Influence on TET3 Expression in Breast Cancer Cell Lines with Distinct Biological Subtypes. *International Journal of Molecular Sciences*, *25*(16), 8561. https://doi.org/10.3390/ijms25168561

Masand, V. H., Al-Hussain, S. A., Alzahrani, A. Y., Al-Mutairi, A. A., Hussien, R. A., Samad, A., & Zaki, M. E. A. (2024). Estrogen Receptor Alpha Binders for Hormone-Dependent Forms of Breast Cancer: e-QSAR and Molecular Docking Supported by X-ray Resolved Structures. *ACS Omega*, *9*(14), 16759–16774. https://doi.org/10.1021/acsomega.4c00906

McDougal, D. P., Pederick, J. L., Novick, S. J., Jovcevski, B., Warrender, A. K., Pascal, B. D., Griffin, P. R., & Bruning, J. B. (2025). A ternary switch model governing ERα ligand binding domain conformation. *Nature Communications*, *16*(1), 10363. https://doi.org/10.1038/s41467-025-65323-9

Mills, J. N., Rutkovsky, A. C., & Giordano, A. (2018). Mechanisms of resistance in estrogen receptor positive breast cancer: overcoming resistance to tamoxifen/aromatase inhibitors. *Current Opinion in Pharmacology*, *41*, 59–65. https://doi.org/10.1016/j.coph.2018.04.009

Mora Lagares, L., Minovski, N., Caballero Alfonso, A. Y., Benfenati, E., Wellens, S., Culot, M., Gosselet, F., & Novič, M. (2020). Homology Modeling of the Human P-glycoprotein (ABCB1) and Insights into Ligand Binding through Molecular Docking Studies. *International Journal of Molecular Sciences*, *21*(11), 4058. https://doi.org/10.3390/ijms21114058

Salmaso, V., & Moro, S. (2018). Bridging Molecular Docking to Molecular Dynamics in Exploring Ligand-Protein Recognition Process: An Overview. *Frontiers in Pharmacology*, *9*. https://doi.org/10.3389/fphar.2018.00923

Santos-Martins, D., Solis-Vasquez, L., Tillack, A. F., Sanner, M. F., Koch, A., & Forli, S. (2021). Accelerating AutoDock 4 with GPUs and Gradient-Based Local Search. *Journal of Chemical Theory and Computation*, *17*(2), 1060–1073. https://doi.org/10.1021/acs.jctc.0c01006

Shiau, A. K., Barstad, D., Loria, P. M., Cheng, L., Kushner, P. J., Agard, D. A., & Greene, G. L. (1998). The Structural Basis of Estrogen Receptor/Coactivator Recognition and the Antagonism of This Interaction by Tamoxifen. *Cell*, *95*(7), 927–937. https://doi.org/10.1016/S0092-8674(00)81717-1

Suzuki, A., Shirota, O., Mori, K., Sekita, S., Fuchino, H., Takano, A., & Kuroyanagi, M. (2009). Leishmanicidal Active Constituents from Nepalese Medicinal Plant Tulsi (Ocimum sanctum L.). *Chemical and Pharmaceutical Bulletin*, *57*(3), 245–251. https://doi.org/10.1248/cpb.57.245

Tanenbaum, D. M., Wang, Y., Williams, S. P., & Sigler, P. B. (1998). Crystallographic comparison of the estrogen and progesterone receptor's ligand binding domains. *Proceedings of the National Academy of Sciences*, *95*(11), 5998–6003. https://doi.org/10.1073/pnas.95.11.5998

Tian, C., Kasavajhala, K., Belfon, K. A. A., Raguette, L., Huang, H., Migues, A. N., Bickel, J., Wang, Y., Pincay, J., Wu, Q., & Simmerling, C. (2020). ff19SB: Amino-Acid-Specific Protein Backbone Parameters Trained against Quantum Mechanics Energy Surfaces in Solution. *Journal of Chemical Theory and Computation*, *16*(1), 528–552. https://doi.org/10.1021/acs.jctc.9b00591

Vajdos, F. F., Hoth, L. R., Geoghegan, K. F., Simons, S. P., LeMotte, P. K., Danley, D. E., Ammirati, M. J., & Pandit, J. (2007). The 2.0 Å crystal structure of the ERα ligand-binding domain complexed with lasofoxifene. *Protein Science*, *16*(5), 897–905. https://doi.org/10.1110/ps.062729207

Wu, B.-X., Wu, H.-T., Lan, Y.-Z., Chen, W.-J., Yu, X.-N., Liu, J.-W., & Liu, J. (2025). Targeting estrogen receptor alpha in breast cancer for novel therapies resistance mechanisms and future directions. *Discover Oncology*. https://doi.org/10.1007/s12672-025-04302-4

Yao, J., Tao, Y., Hu, Z., Li, J., Xue, Z., Zhang, Y., & Lei, Y. (2023). Optimization of small molecule degraders and antagonists for targeting estrogen receptor based on breast cancer: current status and future. *Frontiers in Pharmacology*, *14*. https://doi.org/10.3389/fphar.2023.1225951

Yusuff, O. K., Omotosho, K., & Raji, A. T. (2023). COMPARATIVE CHAINS DYNAMICS OF TRIOSEPHOSPHATE ISOMERASE INVESTIGATED BY MOLECULAR DYNAMICS SIMULATION. *Journal of Chemical Society of Nigeria*, *48*(1). https://doi.org/10.46602/jcsn.v48i1.856

Zhang, D., & Lazim, R. (2017). Application of conventional molecular dynamics simulation in evaluating the stability of apomyoglobin in urea solution. *Scientific Reports*, *7*(1), 44651. https://doi.org/10.1038/srep44651